Published online 28 December 2012 *Nucleic Acids Research, 2013, Vol. 41, No. 3* ***1637–1648***
doi:10.1093/nar/gks1440

Decoupling nucleosome recognition from DNA binding dramatically alters the properties of the Chd1 chromatin remodeler

Ashok Patel, Srinivas Chakravarthy, Seamus Morrone, Ilana M. Nodelman, Jeffrey N. McKnight and Gregory D. Bowman*

T.C. Jenkins Department of Biophysics, Johns Hopkins University, Baltimore, MD 21218, USA

Received August 30, 2012; Revised December 7, 2012; Accepted December 9, 2012

ABSTRACT

Chromatin remodelers can either organize or disrupt nucleosomal arrays, yet the mechanisms specifying these opposing actions are not clear. Here, we show that the outcome of nucleosome sliding by Chd1 changes dramatically depending on how the chromatin remodeler is targeted to nucleosomes. Using a Chd1–streptavidin fusion remodeler, we found that targeting via biotinylated DNA resulted in directional sliding towards the recruitment site, whereas targeting via biotinylated histones produced a distribution of nucleosome positions. Remarkably, the fusion remodeler shifted nucleosomes with biotinylated histones up to 50 bp off the ends of DNA and was capable of reducing negative supercoiling of plasmids containing biotinylated chromatin, similar to remodelling characteristics observed for SWI/SNF-type remodelers. These data suggest that forming a stable attachment to nucleosomes via histones, and thus lacking sensitivity to extranucleosomal DNA, seems to be sufficient for allowing a chromatin remodeler to possess SWI/SNF-like disruptive properties.

INTRODUCTION

Nucleosomes, the basic chromatin packaging unit in eukaryotes, block ready access to genomic DNA. Thus, nucleosome placement, organization and occupancy impact the ability of cellular machinery to carry out basic processes, such as DNA replication, recombination, repair and gene transcription (1–3). Nucleosomes are actively and dynamically reorganized by several subfamilies of adenosine triphosphate (ATP)-driven machines called chromatin remodelers. Although all remodelers share a common highly conserved ATPase motor, each subfamily is found with a unique collection of auxiliary domains and subunits that seem to confer distinct biochemical activities (4,5). SWI/SNF-type remodelers, which often participate in activating gene transcription, have been shown to promote nucleosome disassembly both *in vitro* and *in vivo* (6–12). Chd1 and Iswi-type remodelers, in contrast, promote nucleosome assembly and help establish and maintain regularly spaced nucleosome arrays (13–15).

Although differing in the outcome of their remodelling reactions, these three subfamilies of remodelers share the ability to reposition or 'slide' nucleosomes along DNA. Consistent with their propensity for disorganizing nucleosomal arrays, SWI/SNF-type remodelers can slide nucleosomes irrespective of extranucleosomal DNA, resulting in histone octamers moving off the ends of DNA *in vitro* (16,17). Such movement of mononucleosomes off DNA ends exposes part of the histone core and may underlie the characteristic abilities of SWI/SNF-type remodelers to reorganize mononucleosomes into non-covalent dimers, promote histone exchange with free DNA and other nucleosomes in trans and destabilize the histone core (6,18–20). On polynucleosome templates, SWI/SNF-type remodelers can slide nucleosomes into territories of neighbouring nucleosomes, and this activity has been proposed to be a primary means for unwrapping and disassembling histones from DNA (7). By partially unwrapping neighbouring nucleosomes, collisions between nucleosomes are believed to give rise to dinucleosome-like assemblies called altosomes, which have altered DNA accessibility and reduced negative writhe of DNA associated with canonical nucleosomal wrapping (21–23).

Chd1 and Iswi-type remodelers differ dramatically from SWI/SNF-type remodelers, with their sliding activities

*To whom correspondence should be addressed. Tel: +1 410 516 7850; Fax: +1 410 516 4118; Email: gdbowman@jhu.edu
Present addresses:
Srinivas Chakravarthy, IIT/BioCAT, Sector 18, 9700 S.Cass Avenue, Building 435B, Lemont, IL 60439, USA.
Seamus Morrone, Department of Biophysics and Biophysical Chemistry, Johns Hopkins University School of Medicine, 725 N. Wolfe Street, Baltimore, MD 21205, USA.
Jeffrey N. McKnight, Basic Sciences Division, Fred Hutchinson Cancer Research Center, Seattle, WA 98109, USA.

strongly dependent on the length of DNA flanking the nucleosome. Instead of moving mononucleosomes off the ends of DNA, Chd1 and most Iswi-type remodelers preferentially move nucleosomes away from DNA ends, which results in centring mononucleosomes on short DNA fragments (24–27). The sensitivity of Chd1 and Iswi-type remodelers for DNA flanking the nucleosome (called extranucleosomal DNA) seems to arise from a similar DNA-binding domain located just C-terminal to the ATPase motor. The DNA-binding domains for Chd1 and Iswi both consist of SANT and SLIDE domains that interact with DNA in a sequence–non-specific fashion (28–32). These DNA-binding domains preferentially interact with extranucleosomal DNA, and, in a manner that is not presently understood, bias the remodeler to shift the histone core towards longer stretches of available DNA (25–27). For Chd1, we previously demonstrated that the native DNA-binding domain is not required for nucleosome sliding and can be functionally substituted with foreign sequence-specific DNA-binding domains (33). These fusion Chd1 remodelers were found to slide nucleosomes directionally, suggesting that a primary function of the DNA-binding domain is to tether the rest of the remodeler to the nucleosome substrate. An important question raised by these experiments was how much the dependence on binding to extranucleosomal DNA influenced the outcome of the nucleosome sliding reaction.

Here, we show that changing the manner in which the Chd1 remodeler is tethered to nucleosomes dramatically alters the extent and direction that nucleosomes are shifted. We have substituted the native Chd1 DNA-binding domain with monomeric streptavidin, which allows the remodeler to be tethered to nucleosomes via either biotinylated extranucleosomal DNA or biotinylated histones. Targeting Chd1–streptavidin to nucleosomes with biotinylated DNA resulted in directional movement of nucleosomes onto the target site, resembling sliding previously observed with foreign DNA-binding domains (33). In contrast, targeting Chd1–streptavidin using biotinylated histones resulted in bi-directional movement and allowed the remodeler to move nucleosomes up to 50 bp off the ends of the DNA. Similar to RSC, the fusion remodeler disrupted histone octamers from dinucleosome substrates. On plasmids containing pre-assembled chromatin, Chd1–streptavidin reduced negative supercoiling of chromatinized plasmids in a biotin-dependent manner. The disrupted chromatin slowly regained some negative supercoiling over time, resembling the characteristics of altosomes created by SWI/SNF (21). These findings demonstrate how a non-ATPase domain can direct the outcome of a nucleosome sliding reaction without specific interactions with the rest of the remodeler.

MATERIALS AND METHODS

Production of biochemical reagents

The Chd1–monostreptavidin remodeler (called Chd1[ΔDBD/+mSA]) contained residues 13–140 of streptavidin fused to the C-terminus of a *Saccharomyces cerevisiae* Chd1 construct lacking the DNA-binding domain (residues 118–1014). The streptavidin clone (kindly provided by Matthew Levy) contained five amino acid changes that favour a soluble monomeric form of streptavidin (V55T, T76R, L109T, W120G and V125R), as well as S52G and R53S (34,35). The Chd1 construct containing the native DNA-binding domain (residues 118–1274, called $Chd1_{\Delta NC}$ to indicate N- and C-terminal truncations) possessed the three signature Chd-family motifs (double chromodomains, ATPase motor and DNA-binding domain) and has been shown to slide and preferentially centre mononucleosomes (33,36). Both Chd1[ΔDBD/+mSA] and $Chd1_{\Delta NC}$ proteins were expressed recombinantly in *Escherichia coli* BL21 (DE3) (star) cells using autoinduction methods (37) and purified as previously described for $Chd1_{\Delta NC}$ (36). RSC was purified from yeast strain BCY211 using a TAP-tag protocol targeting Rsc2 as previously described (38,39).

Xenopus laevis histone proteins were expressed, purified and refolded into octamers as previously described (40,41). For generating histone-biotinylated nucleosomes, cysteine variants for histone H2A (T120C) and H3 (A21C; C110A) were labelled with biotin-maleimide (Sigma) following procedures described for fluorescent labelling of histones (42). Nucleosomal DNA contained the 145-bp Widom 601 positioning sequence for mononucleosomes and the 601 and 603 positioning sequences for dinucleosomes (43). DNA fragments were generated by polymerase chain reaction using fluorescently labelled primers (Integrated DNA Technologies, IDT). Biotinylated DNA was generated by polymerase chain reaction, amplifying the desired DNA construct using primers synthesized with biotin-dT or 5′-end labelled biotin (IDT). Fluorescently labelled DNAs were purified by native polyacrylamide gel electrophoresis (PAGE) and reconstituted into nucleosomes by mixing 1:1 (or other ratios as indicated) with histone octamers in 2 M KCl and removing salt by gradient dialysis as described (40,41). After reconstitution, all mono- and dinucleosomes were purified by native PAGE using a mini-prep cell apparatus (Bio-Rad). For chromatinized plasmids, histones were salt (NaCl) gradient dialysed with pJ201(34×601), a 10-kb plasmid containing 34 copies of 601 in 208-bp repeats, or with pGEM601, a 3-kb plasmid with one 601 sequence, in different octamer:DNA ratios (0.1:1.0–1.3:1.0). Considering one histone octamer to 200-bp DNA to be 1:1, optimal saturation was achieved with a DNA:histone ratio of 1:1.2 following the procedures of Routh and Rhodes (44).

Nucleosome sliding and binding reactions

Nucleosome sliding reactions were performed either at room temperature (Chd1) or 30°C (RSC) in sliding buffer [50 mM KCl, 2.5 mM ATP, 5 mM $MgCl_2$, 20 mM Tris–HCl (pH 7.6), 0.1 mM ethylenediaminetetraacetic acid (EDTA), 5% sucrose, 0.1 mg/ml bovine serum albumin (BSA) and 5 mM dithiothreitol (DTT)] as previously described (36). Aliquots of nucleosome sliding reactions (2 μl) were quenched at the indicated times by adding

6 µl of stop solution, which contained 2 mg/ml of 601 array plasmid, 1 mM biotin and 5 mM EDTA. Sliding reactions with dinucleosomes additionally contained 100 ng/µl of salmon sperm carrier DNA, which was necessary to visualize the mononucleosome-sized products. Nucleosome binding reactions were performed equivalently to sliding reactions, except that stop solutions were omitted. Nucleosome species were separated by native acrylamide electrophoresis (5% acrylamide for dinucleosomes, 7% for mononucleosomes, each with 60:1 acrylamide to bis-acrylamide and run in 0.25 × TBE at 150 V for 2–2.5 h), detected by fluorescence using a Typhoon 9410 variable mode imager (GE Healthcare) and analyzed by ImageJ (http://imagej.nih.gov/ij/). All binding and sliding reactions are representative of three or more experiments carried out under similar conditions.

Nucleosome mapping reactions

Nucleosome mapping was performed by labelling histone H2B Cys53 with p-azidophenacyl bromide (APB) following previously established protocols (45,46). APB labelling was performed before or after nucleosome repositioning with similar results. After incubation with or without remodelers, APB-labelled nucleosomes were ultraviolet (UV) irradiated to form DNA cross-links, heat- and NaOH-treated to resolve cross-links into DNA nicks and then separated on 8% polyacrylamide (19:1), 8 M urea sequencing gels run at 65 W. Fluorescent DNA was visualized using Typhoon 9410 variable mode imager and ImageJ (http://imagej.nih.gov/ij/), with each nicked position indicative of histone octamer placement on DNA.

Restriction enzyme digestion

Restriction digests using HhaI were carried out using the pJ201 (34 × 601) plasmid pre-assembled with nucleosomes as previously described. $Chd1_{\Delta NC}$ or Chd1[ΔDBD/+mSA] (100 nM) was mixed with the equivalent of 5 nM chromatinized plasmid in buffer 4 + 0.1 mg/ml BSA (New England Biolabs) and incubated for 10 min at 23°C in the presence or absence of 2.5 mM ATP and 5 mM $MgCl_2$ as indicated. One unit of HhaI enzyme was then added and allowed to digest for additional time as indicated at 23°C with continued nucleosome sliding. Restriction digest and sliding reactions (50 µl) were stopped with the addition of 10 µl of stop solution (0.5 M EDTA, 1 µg/ml RNase), 100 µl of Glycogen stop buffer (20 mM EDTA, 0.2 M NaCl, 1% sodium dodecyl sulphate and 0.25 mg/ml of glycogen) and 5 µl of Proteinase K (2.5 mg/ml), incubated at 37°C for 30 min, and then DNA purified with phenol:chloroform extraction. After precipitation with ammonium acetate and isopropanol, DNA samples were visualized on 1.4% agarose gels stained with ethidium bromide.

Supercoiling assays

$Chd1_{\Delta NC}$ (100 nM), Chd1[ΔDBD/+mSA] (100 nM) or Chd1[ΔDBD] (10 µM) were mixed with the equivalent of 5 nM chromatinized plasmid (1.2:1.0 histone:DNA ratio) in buffer containing 50 mM Tris–HCl (pH 7.8), 50 mM KCl, 10 mM $MgCl_2$, 0.1 mM EDTA, 0.1 mg/ml BSA and 1 mM DTT. Reactions (45 µl) were then mixed with 5 µl of *Drosophila melanogaster* topoisomerase I (3.4 µg/ml) and incubated for the indicated times at 28°C. Where indicated, ATP was present at 2.5 mM. For Chd1[ΔDBD/+mSA] samples, reactions were stopped with 10 mM biotin and were either allowed additional time for supercoiling reversion at 28°C, or were immediately quenched with Glycogen stop buffer and Proteinase K and processed as previously described for HhaI reactions. For 1D gels, duplicate samples were applied on two 15 × 15 cm 0.8% agarose gels with or without 2 µg/ml of chloroquine in both the gel and running buffer (1 × TBE). Gels were run at 100 V (3.3 V/cm) for 4 h and then stained with 1 µg/ml of ethidium bromide for 15 min, destained 5 min in water and visualized in UV. For 2D gels, samples were loaded into round wells on 15 × 15 cm 0.8% agarose gels made with 1 × TBE and run at 100 V (3.3 V.cm) for 2 h in 1 × TBE without chloroquine. The gels were, subsequently, soaked in running buffer containing 2 µg/ml of chloroquine for 2 h before running in the second dimension (rotation by 90°) again for 2 h at 100 V with 2 µg/ml of chloroquine in 1 × TBE running buffer. Gels were then stained with 1 µg/ml of ethidium bromide for 15 min, destained 5 min in water and visualized in UV.

RESULTS AND DISCUSSION

The native Chd1 DNA-binding domain can be functionally replaced by monomeric streptavidin

Our previous studies on Chd1 fusion remodelers showed that foreign DNA-binding domains could promote rapid nucleosome sliding by targeting high-affinity sequences on extranucleosomal DNA (33). To further investigate how the nature and location of nucleosome attachment may influence the chromatin remodelling reaction, we designed a Chd1–streptavidin fusion remodeler. We hypothesized that tethering Chd1 through a streptavidin–biotin linkage, if positioned properly, should be able to substitute for attachment of a DNA-binding domain to extranucleosomal DNA. A monomeric form of streptavidin (mSA) (34,35) was used to replace the native Chd1 DNA-binding domain (DBD), generating a fusion remodeler hereafter called Chd1[ΔDBD/+mSA].

To test this fusion remodeler, nucleosome sliding reactions were performed with centrally positioned mononucleosomes possessing or lacking biotin on extranucleosomal DNA (Figure 1). As observed by native PAGE, non-biotinylated mononucleosomes failed to be repositioned by Chd1[ΔDBD/+mSA] in all but the highest concentration and longest time point, consistent with previous observations that truncated Chd1 proteins lacking the DBD are poorly associated with or stimulated by nucleosomes (lanes 1–10) (33). In contrast, mononucleosomes with biotin located +11 or +16 bp from the edge of the nucleosome were more readily repositioned (lanes 11–30). Chd1[ΔDBD/+mSA] bound to the +28 (5′-biotinylated) nucleosomes in a biotin-dependent manner similarly to +11 and +16 biotinylated nucleosomes (Supplementary Figure S1), yet failed to significantly reposition the +28 nucleosomes except at the

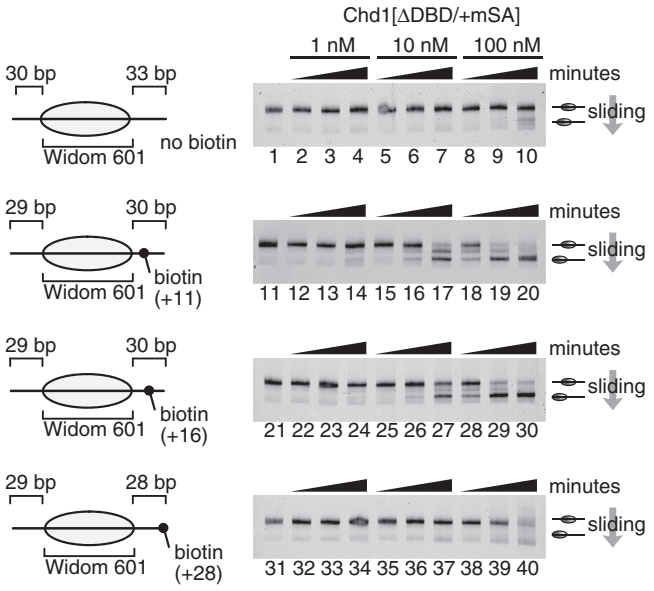

Figure 1. The Chd1–streptavidin remodeler slides nucleosomes in a biotin- and distance-dependent manner. Nucleosome sliding ability of Chd1[ΔDBD/+mSA] was tested using substrates lacking and possessing DNA-conjugated biotin moieties +11, +16 and +28 bp from the edge of the nucleosome. FAM-labelled centred nucleosomes (100 nM) were incubated with the indicated amounts of Chd1[ΔDBD/+mSA] for 0.5, 5 and 50 min under sliding conditions, and the reactions were then stopped with EDTA and free biotin. Reactions were monitored by native PAGE, where faster band migration is indicative of repositioning the histone octamer towards DNA ends.

highest concentration and longest time point (lanes 31–40), indicating that biotin-dependent sliding was distance dependent. This distance dependence was consistent with previous observations of the Chd1[ΔDBD/+AraC] fusion remodeler, which showed a sharp drop in activity when the high-affinity binding site began ≥23 bp from the nucleosome edge (33).

To determine the precise locations where nucleosomes were repositioned, we used the photoactivatable cross-linker APB at position 53 of histone H2B (45,46). For the 145-bp Widom 601 sequence, each APB-modified H2B–Cys53 creates a cross-link with one DNA strand, 18 nucleotides from the edge of the nucleosome (Figure 2A). For the +11 and +16 biotinylated 29-N-30 nucleosomes, cross-links were initially observed 47 nucleotides from the 5′-FAM label, corresponding to 29 nucleotides of extranucleosomal DNA in addition to 18 nucleotides inside the edge of the nucleosome (Figure 2B, lanes 1 and 4). As a control, these nucleosomes were also mapped after sliding with a Chd1 protein possessing the native DBD, called $Chd1_{\Delta NC}$. $Chd1_{\Delta NC}$ preferentially centres mononucleosomes (33,36), and accordingly, the biotinylated nucleosomes showed a distribution about the initial centrally located position (lanes 3 and 6, open arrows). In contrast, Chd1[ΔDBD/+mSA] shifted the histone octamer towards the biotinylated sites, predominantly +19 and +31–35 bp from the starting position (lanes 2 and 5, shaded arrows). Biotinylation of extranucleosomal DNA, therefore, seemed to selectively promote directional sliding by Chd1[ΔDBD/+mSA] (Figure 2C).

A small population of +11 and +16 DNA-biotinylated nucleosomes were shifted +59–62 bp, which means that the histone octamer was moved 29–32 bp off the end of the DNA fragment. Movement of nucleosomes >10 bp off the ends of DNA has previously been observed for SWI/SNF and RSC remodelers, but not for Chd1 or Iswi-type remodelers (6,16,17,27). For Chd1[ΔDBD/+mSA], we wondered whether the much smaller populations of nucleosomes shifted ~30 bp off one DNA end reflected weaker biotin–streptavidin interactions after biotinylated sites were shifted onto the nucleosome.

To compare the relative affinities of Chd1[ΔDBD/+mSA] with nucleosomes before and after sliding, the fusion remodeler was first incubated with DNA-biotinylated nucleosomes for 50 min in the presence of either ATPγS, which prevented sliding, or ATP, which allowed for sliding. After stopping the sliding reactions with EDTA, additional Chd1[ΔDBD/+mSA] was titrated into the reactions, and the levels of remodeler–nucleosome association were evaluated by native PAGE (Figure 2D). ATP-dependent remodelling of DNA-biotinylated nucleosomes produced several faster migrating bands. Comparison of these sliding products with 0-N-63 nucleosomes that were repositioned and mapped (Supplementary Figure S2) suggested that the fastest migrating bands were nucleosomes that had shifted off of DNA ends, and that the slightly slower migrating bands were end-positioned nucleosomes. For both the +11 and +16 nucleosomes, the end-positioned nucleosomes were super-shifted more poorly than the starting material, suggesting that the biotinylation sites were occluded by the nucleosome after sliding. This reduction in binding was more pronounced for +11 nucleosomes than +16 nucleosomes, which likely reflected differences in rotational phasing of the biotinylated site on the nucleosome. It is important to note that unlike the high affinity of wild-type, tetrameric streptavidin for biotin ($K_D \sim 10^{-14}$ M) (47), the monomeric streptavidin variant has a much lower binding affinity ($K_D \sim 10^{-7}$ M) (34,35). This lower binding affinity explains the lack of super-shifted bands at 100 nM remodeler (Figure 2D, lanes 9, 16, 23 and 30) and the smearing at higher concentrations.

An important question raised by these experiments was the extent to which changes in biotin accessibility influenced the distribution of remodelled nucleosome positions. That is, did the chromodomain/ATPase portion of Chd1 have the capability to robustly slide nucleosomes off DNA ends like SWI/SNF-type remodelers, but was effectively unable to do so because of reduced interactions with the substrate?

Targeting Chd1 to histones allows nucleosomes to be shifted up to 50 bp off of DNA ends

The biotin-dependent activity of Chd1[ΔDBD/+mSA] indicated that the nature of the interaction with extranucleosomal DNA was not critical for moving histone octamers along DNA, but rather it suggested

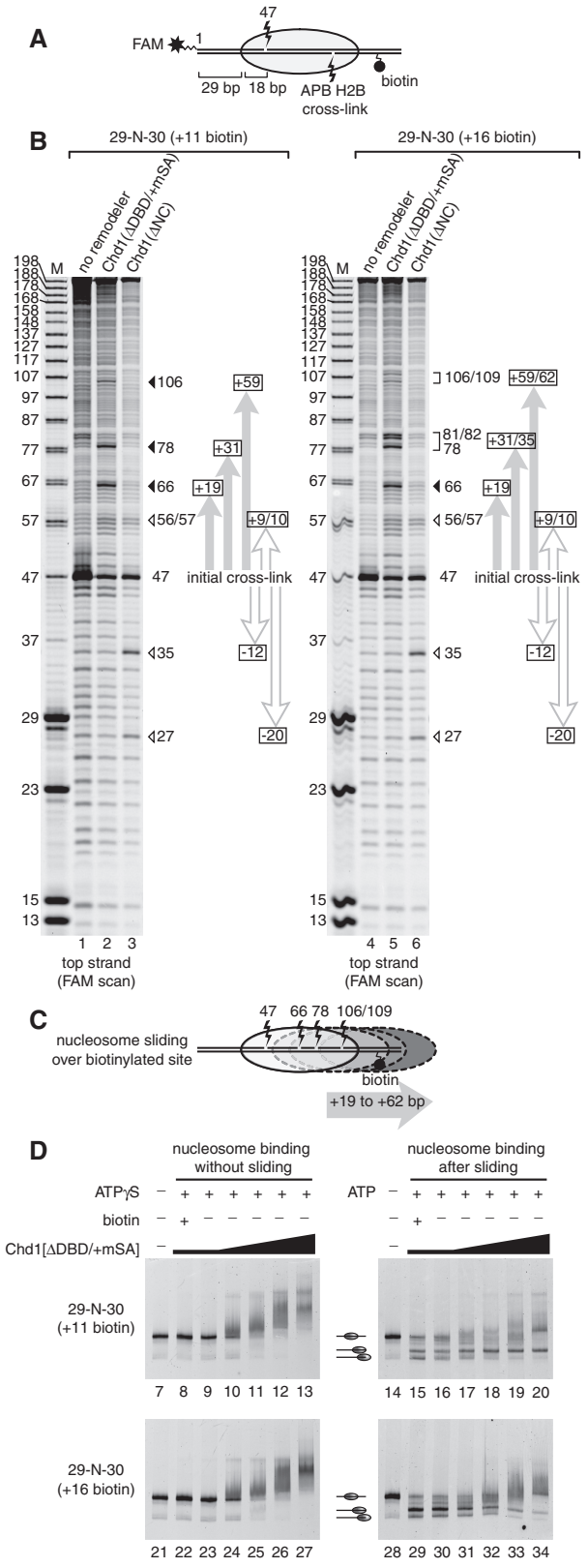

Figure 2. The Chd1–streptavidin remodeler buries biotinylated DNA sites on the nucleosome. (**A**) Schematic of APB-H2B cross-links generated on FAM-labelled 29-N-30 nucleosomes containing biotinylated DNA. Mapping was performed using a Ser53Cys variant of H2B, which forms a single cross-link to each strand, 18 nucleotides 3′ from the edge of the 145-bp Widom 601 sequence, corresponding to 47 bp from the 5′-FAM label of unshifted 29-N-30 nucleosomes.

that tethering the remodeler close to the nucleosome substrate was sufficient for promoting nucleosome sliding. To investigate whether interactions with extranucleosomal DNA could be dispensed with altogether, we generated nucleosomes that were biotinylated on histones. As biotinylated histones should remain exposed throughout the sliding reaction, these substrates were also expected to reveal how continued accessibility of the tether site influences the distribution of remodelled products.

Using biotin-maleimide, we labelled single cysteine residues introduced at amino acid position 120 of histone H2A or position 21 of histone H3 (Figure 3A). These biotinylated histones were separately used to make end-positioned 0-N-63 nucleosomes, and the ability of Chd1[ΔDBD/+mSA] to slide these nucleosomes was evaluated by native PAGE (Figure 3B). Chd1[ΔDBD/+mSA] altered the migration of both H3- and H2A-biotinylated nucleosomes, but unlike nucleosomes with biotinylated DNA, the biotinylated nucleosomes produced somewhat smeary patterns with multiple bands when remodelled, suggesting that the histone octamer was repositioned across a range of locations. To more precisely determine the distribution of octamer positions, histone–DNA contact mapping was used (Figure 3C). Chd1$_{\Delta NC}$, used as a control, showed directional sliding towards the middle of the DNA fragment: the initial histone–DNA cross-linking site at position 81 shifted +19 to +41 bp onto the extranucleosomal DNA (Figure 3D, lanes 22 and 26). In contrast, sliding by Chd1[ΔDBD/+mSA] produced a broad range of octamer positions (lanes 24 and 27, shaded arrows). In addition to repositioning throughout the extranucleosomal DNA, the histone octamer also yielded significant cross-linking 99, 110 and 121/122 bp from the 5′-FAM label, corresponding to shifts of −18, −29 and −40/41 bp, respectively, off the '0' end of the DNA fragment (Figure 3E).

To further characterize the remodelled products, we performed large-scale sliding reactions with biotinylated H2A nucleosomes and purified the three major nucleosome species apparent by native PAGE (Supplementary Figure S2). Mapping these three species revealed that the nucleosomes that migrated the fastest by native PAGE

Figure 2. Continued
(**B**) Histone–DNA contact mapping reactions. All reactions contained 150 nM nucleosomes and 0 or 50 nM remodeler as indicated and they were carried out at room temperature with 2 mM ATP and 5 mM $MgCl_2$ for 20 min. Cross-linking sites for Chd1[ΔDBD/+mSA] are labelled with filled arrowheads and brackets, which were only observed in the direction of the biotinylated DNA sites (shaded arrows). Cross-linking sites for Chd1$_{\Delta NC}$ are labelled by open arrowheads and were observed on either side of the initial cross-link position (white arrows). (**C**) A cartoon representation of the cross-links and corresponding positions of the histone octamer on the DNA after sliding by Chd1[ΔDBD/+mSA]. (**D**) Nucleosomes with biotinylated DNA associated with Chd1[ΔDBD/+mSA] more poorly after sliding. To compare binding before and after sliding, DNA-biotinylated nucleosomes (100 nM) were first incubated with Chd1[ΔDBD/+mSA] (100 nM) at room temperature in the presence of ATPγS (no sliding) or ATP (sliding), as indicated. After 50 min, EDTA was then added to all reactions, and biotin was added as indicated. The reactions were then placed on ice for 2 h after additional Chd1[ΔDBD/+mSA] was added to yield final concentrations of 0, 100, 100, 200, 400, 600 and 800 nM remodeler and then analysed by native PAGE.

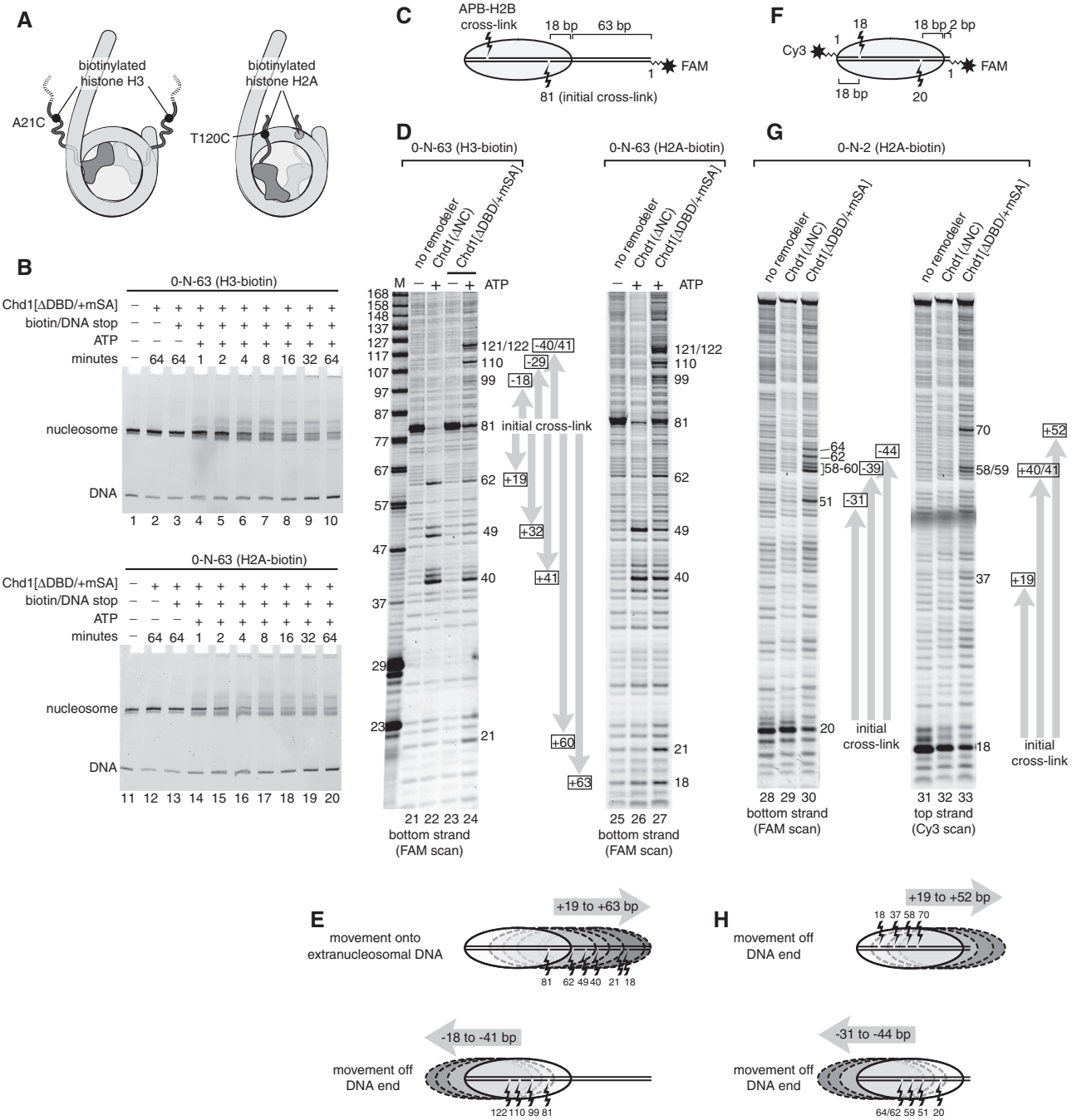

Figure 3. The Chd1–streptavidin remodeler can move nucleosomes off the ends of DNA and independently of extranucleosomal DNA. (**A**) Schematic of nucleosomes showing biotinylation sites on flexible histone tails. (**B**) FAM-labelled nucleosomes (150 nM) containing biotinylated H3 (top) or H2A (bottom) were incubated with Chd1[ΔDBD/+mSA] (50 nM) in sliding buffer with or without ATP for the indicated times, and then stopped with EDTA and excess free biotin. (**C**) Schematic showing the locations of initial cross-links for the FAM-labelled 0-N-63 nucleosome. (**D**) Histone–DNA contact mapping was used to determine the locations of the histone octamer for 0-N-63 nucleosomes before and after sliding with Chd1$_{\Delta NC}$ and Chd1[ΔDBD/+mSA]. With biotinylated histones, cross-links were observed throughout the DNA fragment, with negative numbers (−18, −29, −40/41), indicating the distances shifted off of the '0' DNA end, and positive numbers (+19 to +63), indicating the distances shifted onto extranucleosomal DNA. Mapping with H2B-Cys53 prevented visualization of octamer movement off the 5′-FAM labelled end, as the cross-linking residue loses contact with DNA. However, movement off of the FAM-labelled DNA end was confirmed by monitoring the Cy3-labelled top strand (not shown). (**E**) Schematic representations for the mapping reactions shown in (D), highlighting the histone octamer locations and corresponding cross-links of the 0-N-63 nucleosome after sliding with Chd1[ΔDBD/+mSA]. (**F**) Schematic showing the locations of cross-links for the double-labelled FAM/Cy3 0-N-2 nucleosome. (**G**) Histone–DNA contact mapping as performed in (D), using 0-N-2 H2A-biotinylated nucleosomes. Mapping is shown for both the bottom strand (FAM-labelled) and top strand (Cy3-labelled). Shaded arrows indicate the distances that the octamer was shifted from the starting position. (**H**) Schematic representations for the directions and magnitude of sliding for mapping reactions of 0-N-2 nucleosomes shown in (G).

corresponded to those that were shifted off the ends, which is consistent with what has been observed with nucleosomes remodelled by SWI/SNF and RSC (6,7,16,17). We were unable to conclusively determine whether nucleosomes that were shifted off DNA ends were partially disassembled (e.g. loss of one H2A/H2B dimer, or part of H3/H4 tetramer). However, as histone mapping requires the proper positioning of Cys53 of H2B, it is unlikely that partial disassembly alone accounts for the new cross-linked positions.

The lack of sliding directionality and the significant distribution of remodelled products off DNA ends suggested that attachment of Chd1[ΔDBD/+mSA] to nucleosomes via histones made the remodeler insensitive to extranucleosomal DNA. To further examine how sensitivity to extranucleosomal DNA affected the outcome of nucleosome sliding, Chd1[ΔDBD/+mSA] and $Chd1_{\Delta NC}$ remodelers were independently incubated with H2A-biotinylated nucleosomes made with a 147-bp DNA fragment (0-N-2; Figure 3F). Under sliding conditions, no significant shifts in the cross-link location of 0-N-2 nucleosomes were observed compared with the starting material in the presence of $Chd1_{\Delta NC}$, even up to micromolar concentrations of remodeler (Figure 3G, lanes 29 and 32; data not shown). Although 0-N-2 nucleosomes effectively lack extranucleosomal DNA, these nucleosomes formed super-shifted complexes with $Chd1_{\Delta NC}$ by native PAGE (Supplementary Figure S3), suggesting that the apparent lack of sliding was not because of an inability to bind. While these experiments only report that $Chd1_{\Delta NC}$ does not stably slide 0-N-2 nucleosomes to new positions, it is possible that nucleosomes are transiently repositioned away from the starting location and then back again. This situation may be similar to what has been reported for human ACF, where nucleosome sliding dynamically allowed access to a cleavage site that was occluded by a centrally positioned histone core while maintaining the majority of nucleosomes in a central location on DNA (26).

In contrast to $Chd1_{\Delta NC}$, Chd1[ΔDBD/+mSA] generated a range of new cross-linked products, all of which indicated that the histone octamer was shifted off the DNA ends (Figure 3G, lanes 30 and 33). The maximum distance that the nucleosomes were shifted off the DNA ends was 50 bp (+52 bp in the direction of the '2' side of 0-N-2 nucleosomes; Figure 3H). This approximately equals the maximum distance that nucleosomes can be shifted off DNA ends by SWI/SNF and RSC remodelers (6,16,17) and corresponds to relocating one end of DNA to an internal position on the nucleosome, ~20 bp from the dyad, where the ATPase motors of remodelers engage nucleosomal DNA (48–50).

These results indicate that the ATPase motor of Chd1 has an intrinsic ability to slide nucleosomes off the ends of DNA, but is normally limited by its DBD, which biases sliding towards longer stretches of extranucleosomal DNA. In agreement with others (27), the dependence of the ATPase motor on the DBD provides a means for regulating the extent of nucleosome sliding based on the presence or availability of extranucleosomal DNA.

The Chd1–streptavidin fusion remodeler can disrupt the canonical nucleosomal wrapping of DNA around the histone core in dinucleosome substrates and chromatin arrays

For SWI/SNF, the ability to slide nucleosomes into each other has been proposed to promote eviction of histone octamers (7) and is likely responsible for alternative histone–DNA structures with increased DNA accessibility and altered DNA topologies (51–53). Given the similar abilities of Chd1[ΔDBD/+mSA] and SWI/SNF-type remodelers for sliding mononucleosomes off the ends of a DNA fragment, we sought to determine whether the Chd1–streptavidin fusion remodeler might also be disruptive to multi-nucleosome substrates.

Using a tandem 601–603 template, we generated dinucleosome substrates with non-biotinylated and biotinylated histone H2A and monitored nucleosome remodelling reactions by native PAGE. As expected, $Chd1_{\Delta NC}$ did not disrupt dinucleosomes (Supplementary Figure S4A). Incubating non-biotinylated dinucleosomes with Chd1[ΔDBD/+mSA] and ATP did not produce any significant changes in migration patterns (Supplementary Figure S4B), consistent with the fusion remodeler requiring a tethering point on the nucleosome for robust remodelling activity. In contrast, incubating H2A-biotinylated nucleosomes with Chd1[ΔDBD/+mSA] and ATP produced several new species that migrated faster than dinucleosomes but slower than free DNA (Figure 4A). A similar pattern was observed when dinucleosomes were remodelled by yeast RSC (Figure 4B), which resembled the previously reported dinucleosome remodelling by SWI/SNF (7). For SWI/SNF, the increase in migration speed was shown to correlate with a loss in histones, with the faster migrating band corresponding to mononucleosomes (7). To evaluate whether Chd1[ΔDBD/+mSA] may also be transforming dinucleosomes into mononucleosomes, we compared the profile of the faster migrating species with two types of mononucleosomes. Similar to the strategy of Owen-Hughes and colleagues (23), we mixed histone octamers with the dinucleosome DNA template at different ratios to obtain free DNA, mononucleosomes and dinucleosomes. The faster migrating band observed with 0.5:1 and 1:1 octamer:DNA ratios, which we interpreted to be mononucleosomes, migrated at approximately the same position as the dinucleosome remodelling product generated by Chd1[ΔDBD/+mSA] (Figure 4C, compare lanes 22 and 23 with 26 and 27). We additionally generated end-positioned mononucleosomes using just a single 601 positioning sequence and a DNA fragment corresponding to the same size as that used to make dinucleosomes. These mononucleosomes also migrated at the same rate as the remodelled dinucleosome product (compare lanes 27 and 28), further supporting the interpretation that Chd1[ΔDBD/+mSA] was transforming dinucleosomes into mononucleosomes.

The ejection of one histone core from dinucleosome substrates may have resulted from collisions between two neighbouring nucleosomes, movement of one nucleosome off a DNA end or some combination of the two.

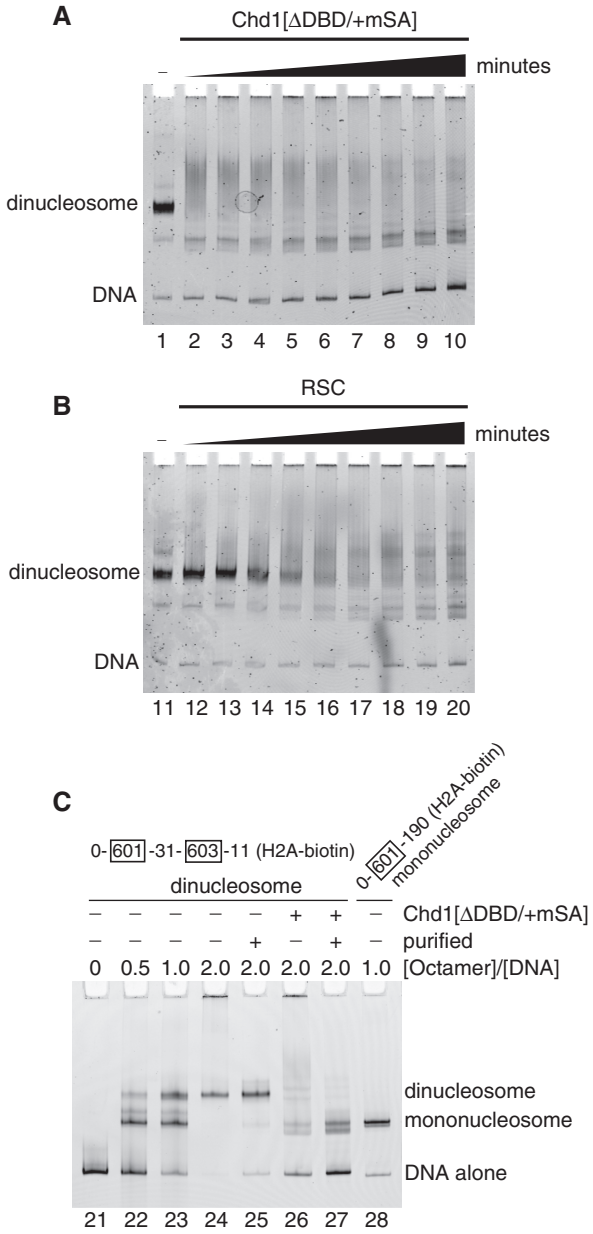

Figure 4. The Chd1–streptavidin remodeler can disrupt histone octamers from dinucleosome substrates. (**A**) Chd1[ΔDBD/+mSA] (200 nM) was incubated with 0-[601]-31-[603]-11 dinucleosomes containing biotinylated H2A (100 nM) at 30°C in sliding buffer, and reactions were stopped after 0.5, 1, 2, 4, 8, 16, 32, 64 and 128 min. (**B**) A sliding reaction carried out under the same conditions as in (A), but using 200 nM yeast RSC. The sliding gels shown in (A) and (B) are representative of three or more experiments carried out under similar conditions. (**C**) Analysis of mono- and dinucleosome products by native PAGE. Lanes 21–24 show various octamer:DNA ratios using the dinucleosome DNA template and histone octamers containing biotinylated H2A. Purified dinucleosomes used for sliding reactions are shown in lane 25. The result of remodelling these purified dinucleosomes (100 nM) with Chd1[ΔDBD/+mSA] (100 nM) for 30 min is shown in lane 26. Purification of the remodelling reaction to enrich for faster migrating species is shown in lane 27, the top band of which corresponds well to migration of end-positioned 0-N-190 mononucleosomes (lane 28).

Notably, Chd1[ΔDBD/+mSA] increased the amount of free DNA from both mono- and dinucleosome substrates containing biotinylated histones, but not mononucleosomes with biotinylated DNA (Figures 3B and 4A; data not shown). The creation of free DNA is consistent with the idea that repositioning nucleosomes off the ends of DNA destabilizes the core. Indeed, destabilization of mononucleosomes has been observed for SWI/SNF-type remodelers, correlating with movement of nucleosomes past DNA ends (6,54). However, in addition to mononucleosome-sized species, Chd1[ΔDBD/+mSA] and RSC remodelers also produced a smear of slower migrating species from dinucleosome substrates, which were not observed with mononucleosome substrates. Although their precise nature is unclear, these species likely resulted from disrupted histones of the dinucleosome substrates. Unlike experiments with mononucleosome substrates, the experiments with dinucleosome substrates required salmon sperm DNA to visualize mononucleosome-sized species. Although generation of free histones is one source of aggregation, the persistence of the slower migrating smear of products in the presence of salmon sperm DNA suggests that these species may have resulted from partial exposure of histone surfaces, from unwrapping or alternative wrapping of DNA, that promoted association of other DNA molecules into larger molecular weight complexes.

To determine whether histone–DNA interactions could be disrupted without sliding off of DNA ends, we investigated how Chd1[ΔDBD/+mSA] affected chromatin pre-assembled onto plasmid DNA. Using salt dialysis, nucleosomes were reconstituted onto a closed circular 10-kb plasmid containing 34 copies of the 601 sequence in 208-bp tandem repeats. This chromatinized plasmid was incubated with either $Chd1_{\Delta NC}$ or Chd1[ΔDBD/+mSA] remodelers in the presence or absence of ATP, and nucleosome placement was monitored by HhaI restriction digestion (Figure 5A). The HhaI recognition sequence is located at the dyad of the 601 sequence, which blocks DNA cleavage. HhaI digestion of the naked DNA template revealed a ladder as expected for the 208-bp repeats, whereas the digestion of the chromatinized plasmid yielded little cleavage because of nucleosome protection. Addition of either $Chd1_{\Delta NC}$ or Chd1[ΔDBD/+mSA] with HhaI resulted in a laddering pattern in an ATP-dependent manner, indicating significant reorganization of nucleosomes to expose the restriction sites.

The HhaI sensitivity on treatment with remodelers and ATP could have resulted from sliding and/or disruption of DNA wrapping around the histone core. To distinguish between these possibilities, a supercoiling assay was used (Figure 5B). In this assay, nucleosomal wrapping maintains negative supercoiling of DNA despite the presence of topoisomerase I. Consistent with previous studies (14), the supercoiled state of plasmid DNA with pre-assembled chromatin was not affected by $Chd1_{\Delta NC}$ (lanes 31–36), indicating that nucleosomes remained intact despite active repositioning that exposed HhaI sites. In contrast, Chd1[ΔDBD/+mSA] stimulated a loss of supercoiling in an ATP-dependent manner (compare lanes 38 and 39 with 41 and 42). This loss in supercoiling was dependent on

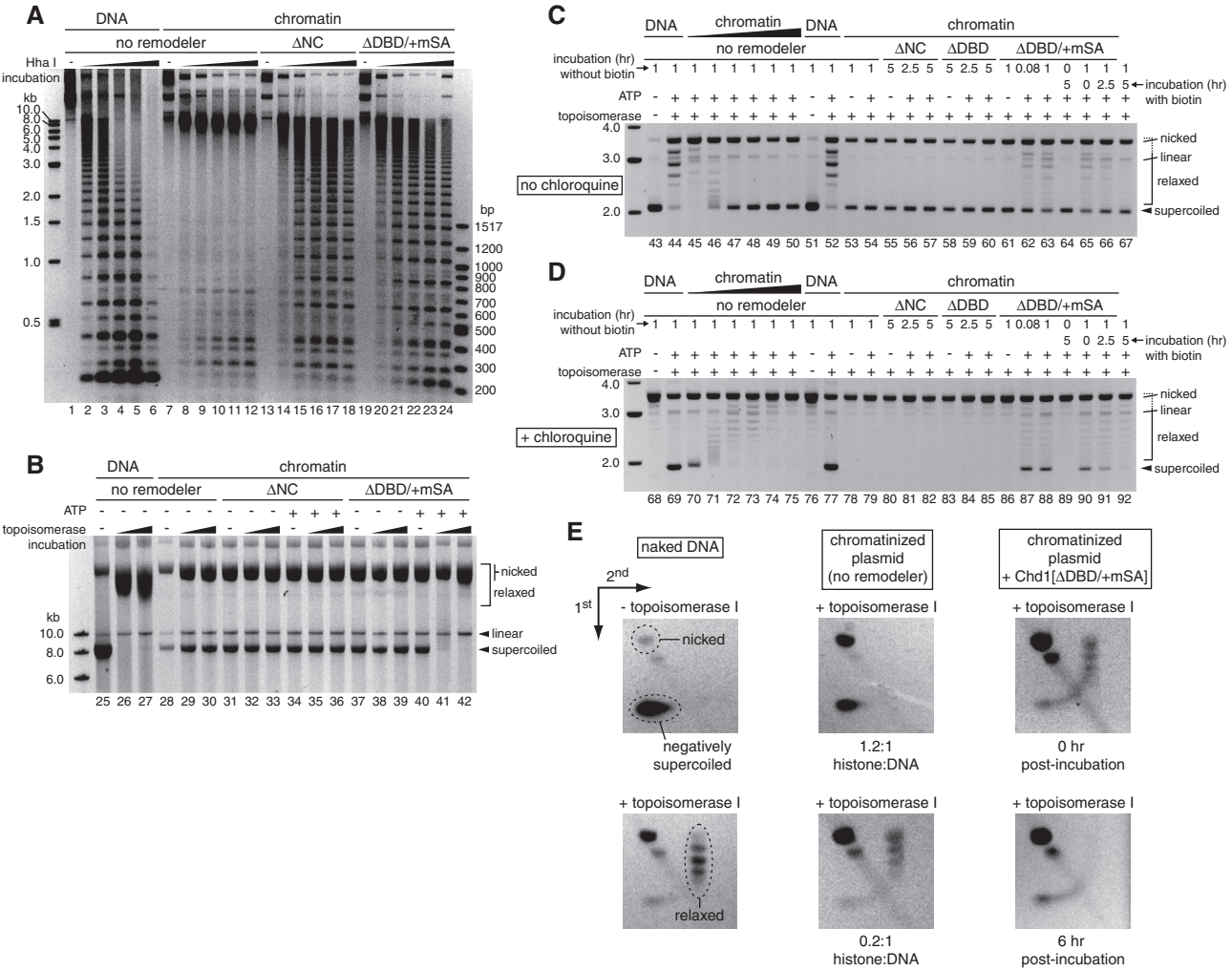

Figure 5. The Chd1–streptavidin remodeler disrupts nucleosomal wrapping of DNA on chromatinized plasmids. (**A**) Both Chd1$_{\Delta NC}$ and Chd1[ΔDBD/+mSA] exposed HhaI sites on pre-assembled nucleosomal arrays. A plasmid containing 34 repeats of the 601 array, with or without pre-assembled nucleosomes (5 nM), was incubated without or with remodelers (100 nM) for 10 min, and then either an additional 25 min without Hha I enzyme (−), or for 5, 10, 15, 20 or 25 min with 1 U of Hha I enzyme. (**B**) Chd1[ΔDBD/+mSA] caused a loss in supercoiling, suggestive of histone disruption. The 10-kb 34-repeat plasmid, with or without pre-assembled nucleosomes, was incubated with or without remodelers for 10 min, and then either another 50 min without topoisomerase (−), or 5 or 50 min with topoisomerase ('topo incubation'). (**C**) Analysis of plasmid supercoiling for a 3-kb template in the presence and absence of nucleosomes and various remodelers. A 3-kb plasmid was incubated with or without topoisomerase as naked DNA (lanes 43, 44, 51 and 52) or after pre-assembly into chromatin in various histone : DNA ratios (0.3, 0.5, 0.7, 0.9, 1.1 and 1.3:1.0 for lanes 45–50, and 1.2:1.0 for lanes 53–67). Pre-assembled chromatin samples incubated with Chd1$_{\Delta NC}$ (100 nM) or Chd1[ΔDBD] (10 μM) were quenched with EDTA, sodium dodecyl sulphate and proteinase K after the indicated times. Reactions with Chd1[ΔDBD/+mSA] (100 nM) were stopped with 10 mM biotin and either immediately quenched or allowed additional incubation time for supercoiling reversion. (**D**) Duplicate samples for reactions shown in (C) analysed in the presence of 2 μg/ml chloroquine. (**E**) Analysis of topoisomers by 2D agarose gel electrophoresis. Samples were electrophoresed first in the absence (first dimension) and then the presence (second dimension) of 2 μg/ml chloroquine. Left panels show the locations of supercoiled, relaxed and nicked species obtained with naked DNA in the presence and absence of topoisomerase. Middle panels show supercoiled and relaxed species of saturated (top) and unsaturated (bottom) chromatinized plasmids, respectively. Right panels show distributions of supercoiled species after 1 h incubation with Chd1[ΔDBD/+mSA] followed by either 0 (top) or 6 h (bottom) additional time for supercoiling reversion.

having nucleosomes with biotinylated histones (data not shown), indicating that relaxation of the plasmid was not simply due to ATP-dependent DNA nicking.

To better observe the relaxed topoisomers, we pre-assembled nucleosomes onto a smaller, 3-kb plasmid, which contained a single 601 sequence. Treatment of this chromatinized plasmid with Chd1[ΔDBD/+mSA] and ATP yielded a pattern of relaxed topoisomers that resembled free plasmid in the presence of topoisomerase I (Figure 5C, lanes 62–63). In the supercoiling reactions, a significant fraction of the template was nicked, making it difficult to estimate the extent that relaxed topoisomers were generated. Supercoiling was therefore examined in the presence of chloroquine, a DNA intercalator that relaxes negatively supercoiled DNA and positively supercoils relaxed (but not nicked) plasmids (Figure 5D). In the presence of chloroquine, Chd1[ΔDBD/+mSA] produced supercoiled species with the same migration as relaxed

plasmid DNA (compare lanes 69 and 77 with 87 and 88), confirming that the remodeler was effectively disrupting the negative supercoils stabilized by nucleosomes. For comparison, we also assembled chromatin with varying histone:DNA ratios (0.1:1.0–1.3:1.0; lanes 45–50, 70–75; data not shown). For these samples, only histone:DNA ratios <0.4:1.0 showed significant levels of relaxed plasmid, suggesting that a significant fraction of nucleosomes were disrupted by Chd1[ΔDBD/+mSA].

Disruption of negative supercoiling for closed circular plasmids containing chromatin is a hallmark of SWI/SNF-type remodelers (51,55,56). Although SWI/SNF has been shown to catalyse the transfer of histones from chromatin to acceptor DNA (6,19,20), changes in plasmid topology do not require histone removal, but instead, can reflect nucleosome reorganization into kinetically trapped states (21,53). These alternative structures, called altosomes, slowly revert back over time to negatively supercoiled states, and thus indicate recovery of nucleosome-like wrapping of DNA. To see whether Chd1[ΔDBD/+mSA] also generated altosome-like structures, we looked for changes in plasmid topology after stopping remodelling activity. As Chd1[ΔDBD/+mSA] was dependent on biotinylated substrates, we used excess biotin to stop remodelling activity, which effectively blocked changes in supercoiling when added before initiating the remodelling reactions (lanes 64 and 89). After stopping with biotin, the changes in plasmid topology from 1 h treatment with Chd1[ΔDBD/+mSA] seemed to slowly reverse, resulting in recovery of negative supercoiling (compare lanes 66 and 67 with 65) concomitant with loss of relaxed topology as detected by chloroquine-induced positive supercoiling (compare lanes 91 and 92 with 90). To confirm the changes in distribution of supercoiled species, we analysed samples with 2D agarose gel electrophoresis (Figure 5E). For these experiments, running plasmid DNA samples in the first and second dimensions in the absence and presence of chloroquine, respectively, separated nicked plasmid from relaxed and negatively supercoiled DNA, distributed in an arcing pattern. As shown in the right panels of Figure 5E, remodelling by Chd1[ΔDBD/+mSA] caused a significant fraction of the chromatin to migrate as relaxed plasmid (top right panel), and a 6 h incubation after addition of biotin changed the distribution of topoisomers back to predominantly a negatively supercoiled state (bottom right panel). Although plasmid nicking reduced the amounts of closed circular plasmid at long incubations, the redistribution towards supercoiled plasmids was suggestive that altosome-like structures were produced by Chd1[ΔDBD/+mSA].

Unlike Chd1[ΔDBD/+mSA], disruption of nucleosome-stabilized DNA supercoiling was not observed for $Chd1_{\Delta NC}$ or Chd1[ΔDBD] remodelers (Figure 5B–D). Chd1 is known for preferentially shifting nucleosomes away from DNA ends or other nucleosomes, resulting in centred mononucleosomes and evenly spaced nucleosome arrays (14,27,33). This preference for moving nucleosomes away from each other is consistent with an inability to disrupt histones via collisions. Chd1[ΔDBD] does not slide nucleosomes directionally (33), yet nucleosome disrupting activity was not apparent. As fusion of streptavidin onto Chd1[ΔDBD] conveyed biotin-dependent, histone disruptive properties, the significantly lower affinity and transient interactions of Chd1[ΔDBD] with nucleosome substrates must have been insufficient for shifting nucleosomes into each other in the experiments presented here. Taken together, these experiments suggest that, although the naturally disruptive remodelers, such as SWI/SNF and RSC, presumably have specialized domains to aid in histone displacement (7,57), disrupting canonical histone–DNA interactions can be achieved simply by tethering a remodeler to nucleosomes independently of DNA flanking the nucleosome core.

CONCLUSIONS

A central conclusion of the work presented here is that a nucleosome-binding domain can guide the outcome of the remodelling reaction without specific contacts with the ATPase motor. Using the Chd1–streptavidin fusion remodeler, we show that the outcomes of remodelling reactions were determined by the manner in which the remodeler was tethered to the nucleosome substrate. When tethered via biotinylated DNA, Chd1[ΔDBD/+mSA] shifted nucleosomes towards its binding site, which resulted in burial and an apparent reduction in affinity towards the biotinylated site (Figure 2). In contrast, when tethered via biotinylated histones, Chd1[ΔDBD/+mSA] robustly shifted nucleosomes off the ends of DNA (Figure 3) and, presumably through nucleosome collisions, disrupted canonical histone–DNA interactions in nucleosome arrays (Figure 5). These dramatic differences revealed that the outcome of nucleosome sliding depends on whether remodeler affinity changes during the course of the reaction. With a dependence on DNA flanking the nucleosome for binding, affinity and, therefore, activity decreased as the binding site became buried by the nucleosome. Tethering the remodeler in a DNA-independent manner, in contrast, allowed the remodeler to continue sliding nucleosomes even when free DNA was no longer available outside the nucleosome core.

Basic classifications of remodelers as organizing or disruptive seem to correlate with whether a remodeler is sensitive to DNA outside the nucleosome. For the natural Chd1 remodeler, tethering depends on a sequence non-specific DNA-binding domain. Like Iswi, this DNA-binding domain promotes directional sliding towards longer available segments of DNA flanking the nucleosome, which shortens the length of DNA bound by the DNA-binding domain (25–27). Sensitivity of the DNA-binding domain to DNA length, therefore, provides a natural feedback mechanism for Chd1 and Iswi-type remodelers that guards against shifting nucleosomes into their neighbours. Alternatively, the insensitivity of SWI/SNF and RSC remodelers for extranucleosomal DNA implies that they depend more strongly on histone-interacting domains, which could continue binding as nucleosomes are shifted close to and

into the territories of their neighbours. Interestingly, a monomeric remodeler closely related to Chd1 called ALC1 (for amplified in liver cancer 1, also known as CHD1L) contains a C-terminal macrodomain that recognizes poly-ADP ribose chains instead of a DNA-binding domain (58,59). Although the fates of polynucleosome templates remodelled by ALC1 have not been reported, tethering via a macrodomain rather than a DNA-binding domain may allow the remodeller to disrupt histone–DNA contacts, consistent with a role in facilitating DNA repair at damaged sites (59,60).

The data presented here also restrict potential mechanisms for how nucleosomes are shifted by remodelers. Previously, it was suggested that different families of remodelers used distinct mechanisms of sliding nucleosomes to account for their unique biochemical properties. For Chd1 and Iswi-type remodelers, which rely on a DBD for recognizing extranucleosomal DNA, the DBD has been proposed to mechanically help the ATPase motor shift DNA past the histone core (29,50,61). We found that Chd1[ΔDBD/+mSA] shifted nucleosomes whether tethered through biotinylated DNA or histones. Thus, although the native Chd1 DBD increases the efficiency of sliding, it seems unlikely to mechanically participate in shifting DNA past the histone core. Instead, our results support a model for nucleosome sliding based on translocation of the ATPase motor. Like SWI/SNF-type remodelers, Chd1[ΔDBD/+mSA] can shift the ends of DNA ~20 bp from the nucleosome dyad, which supports the idea that the ATPase motor shifts DNA past the histone core by translocating at this internal site (48–50). Although a detailed mechanism underlying nucleosome sliding is not presently clear, the biochemical similarities of Chd1[ΔDBD/+mSA] with SWI/SNF-type remodelers suggest that these ATPase motors likely use a common strategy for sliding nucleosomes along DNA.

SUPPLEMENTARY DATA

Supplementary Data are available at NAR Online: Supplementary Figures 1-4.

ACKNOWLEDGEMENTS

The authors thank Matthew Levy for providing the monomeric streptavidin DNA, Karolin Luger for histone expression plasmids, Geeta Narlikar for the histone H2A T120C expression construct, Brad Cairns for the Rsc2-TAP yeast strain for RSC purification, Blaine Bartholomew for the 601/603 dinucleosome template and Jonathan Widom for the 601 sequence. The authors appreciate manuscript reviewers for experimental suggestions, Evan Hass for technical assistance in cloning Chd1[ΔDBD/+mSA] and Kyle Horvath for comments and discussion.

FUNDING

National Institutes of Health [R01 GM084192-5, R01 GM084192-S1 to G.D.B.]. Funding for open access charge: Open Access Promotion Fund of the Johns Hopkins University Libraries.

Conflict of interest statement. None declared.

REFERENCES

1. Kornberg,R.D. and Lorch,Y. (1999) Twenty-five years of the nucleosome, fundamental particle of the eukaryote chromosome. *Cell*, **98**, 285–294.
2. Groth,A., Rocha,W., Verreault,A. and Almouzni,G. (2007) Chromatin challenges during DNA replication and repair. *Cell*, **128**, 721–733.
3. Li,B., Carey,M. and Workman,J.L. (2007) The role of chromatin during transcription. *Cell*, **128**, 707–719.
4. Ryan,D.P. and Owen-Hughes,T. (2011) Snf2-family proteins: chromatin remodellers for any occasion. *Curr. Opin. Chem. Biol.*, **15**, 649–656.
5. Flaus,A., Martin,D.M., Barton,G.J. and Owen-Hughes,T. (2006) Identification of multiple distinct Snf2 subfamilies with conserved structural motifs. *Nucleic Acids Res.*, **34**, 2887–2905.
6. Bruno,M., Flaus,A., Stockdale,C., Rencurel,C., Ferreira,H. and Owen-Hughes,T. (2003) Histone H2A/H2B dimer exchange by ATP-dependent chromatin remodeling activities. *Mol. Cell*, **12**, 1599–1606.
7. Dechassa,M.L., Sabri,A., Pondugula,S., Kassabov,S.R., Chatterjee,N., Kladde,M.P. and Bartholomew,B. (2010) SWI/SNF has intrinsic nucleosome disassembly activity that is dependent on adjacent nucleosomes. *Mol. Cell*, **38**, 590–602.
8. Boeger,H., Griesenbeck,J., Strattan,J.S. and Kornberg,R.D. (2004) Removal of promoter nucleosomes by disassembly rather than sliding in vivo. *Mol. Cell*, **14**, 667–673.
9. Schwabish,M.A. and Struhl,K. (2007) The Swi/Snf complex is important for histone eviction during transcriptional activation and RNA polymerase II elongation in vivo. *Mol. Cell. Biol.*, **27**, 6987–6995.
10. Gkikopoulos,T., Havas,K.M., Dewar,H. and Owen-Hughes,T. (2009) SWI/SNF and Asf1p cooperate to displace histones during induction of the Saccharomyces cerevisiae HO promoter. *Mol. Cell. Biol.*, **29**, 4057–4066.
11. Takahata,S., Yu,Y. and Stillman,D.J. (2009) FACT and Asf1 regulate nucleosome dynamics and coactivator binding at the HO promoter. *Mol. Cell*, **34**, 405–415.
12. Lorch,Y., Griesenbeck,J., Boeger,H., Maier-Davis,B. and Kornberg,R.D. (2011) Selective removal of promoter nucleosomes by the RSC chromatin-remodeling complex. *Nat. Struct. Mol. Biol.*, **18**, 881–885.
13. Ito,T., Bulger,M., Pazin,M.J., Kobayashi,R. and Kadonaga,J.T. (1997) ACF, an ISWI-containing and ATP-utilizing chromatin assembly and remodeling factor. *Cell*, **90**, 145–155.
14. Lusser,A., Urwin,D.L. and Kadonaga,J.T. (2005) Distinct activities of CHD1 and ACF in ATP-dependent chromatin assembly. *Nat. Struct. Mol. Biol.*, **12**, 160–166.
15. Gkikopoulos,T., Schofield,P., Singh,V., Pinskaya,M., Mellor,J., Smolle,M., Workman,J.L., Barton,G.J. and Owen-Hughes,T. (2011) A role for Snf2-related nucleosome-spacing enzymes in genome-wide nucleosome organization. *Science*, **333**, 1758–1760.
16. Kassabov,S.R., Zhang,B., Persinger,J. and Bartholomew,B. (2003) SWI/SNF unwraps, slides, and rewraps the nucleosome. *Mol. Cell*, **11**, 391–403.
17. Flaus,A. and Owen-Hughes,T. (2003) Dynamic properties of nucleosomes during thermal and ATP-driven mobilization. *Mol. Cell. Biol.*, **23**, 7767–7779.
18. Schnitzler,G., Sif,S. and Kingston,R.E. (1998) Human SWI/SNF interconverts a nucleosome between its base state and a stable remodeled state. *Cell*, **94**, 17–27.
19. Lorch,Y., Zhang,M. and Kornberg,R.D. (1999) Histone octamer transfer by a chromatin-remodeling complex. *Cell*, **96**, 389–392.
20. Lorch,Y., Zhang,M. and Kornberg,R.D. (2001) RSC unravels the nucleosome. *Mol. Cell*, **7**, 89–95.

21. Ulyanova,N.P. and Schnitzler,G.R. (2005) Human SWI/SNF generates abundant, structurally altered dinucleosomes on polynucleosomal templates. *Mol. Cell. Biol.*, **25**, 11156–11170.
22. Ulyanova,N.P. and Schnitzler,G.R. (2007) Inverted factor access and slow reversion characterize SWI/SNF-altered nucleosome dimers. *J. Biol. Chem.*, **282**, 1018–1028.
23. Engeholm,M., de Jager,M., Flaus,A., Brenk,R., van Noort,J. and Owen-Hughes,T. (2009) Nucleosomes can invade DNA territories occupied by their neighbors. *Nat. Struct. Mol. Biol.*, **16**, 151–158.
24. Längst,G., Bonte,E.J., Corona,D.F. and Becker,P.B. (1999) Nucleosome movement by CHRAC and ISWI without disruption or trans-displacement of the histone octamer. *Cell*, **97**, 843–852.
25. Kagalwala,M.N., Glaus,B.J., Dang,W., Zofall,M. and Bartholomew,B. (2004) Topography of the ISW2-nucleosome complex: Insights into nucleosome spacing and chromatin remodeling. *EMBO J.*, **23**, 2092–2104.
26. Yang,J.G., Madrid,T.S., Sevastopoulos,E. and Narlikar,G.J. (2006) The chromatin-remodeling enzyme ACF is an ATP-dependent DNA length sensor that regulates nucleosome spacing. *Nat. Struct. Mol. Biol.*, **13**, 1078–1083.
27. Stockdale,C., Flaus,A., Ferreira,H. and Owen-Hughes,T. (2006) Analysis of nucleosome repositioning by yeast ISWI and Chd1 chromatin remodeling complexes. *J. Biol. Chem.*, **281**, 16279–16288.
28. Grüne,T., Brzeski,J., Eberharter,A., Clapier,C.R., Corona,D.F., Becker,P.B. and Müller,C.W. (2003) Crystal structure and functional analysis of a nucleosome recognition module of the remodeling factor ISWI. *Mol. Cell*, **12**, 449–460.
29. Ryan,D.P., Sundaramoorthy,R., Martin,D., Singh,V. and Owen-Hughes,T. (2011) The DNA-binding domain of the Chd1 chromatin-remodelling enzyme contains SANT and SLIDE domains. *EMBO J.*, **30**, 2596–2609.
30. Yamada,K., Frouws,T.D., Angst,B., Fitzgerald,D.J., DeLuca,C., Schimmele,K., Sargent,D.F. and Richmond,T.J. (2011) Structure and mechanism of the chromatin remodelling factor ISW1a. *Nature*, **472**, 448–453.
31. Sharma,A., Jenkins,K.R., Héroux,A. and Bowman,G.D. (2011) Crystal structure of the chromodomain helicase DNA-binding protein 1 (Chd1) DNA-binding domain in complex with DNA. *J. Biol. Chem.*, **286**, 42099–42104.
32. Stokes,D.G. and Perry,R.P. (1995) DNA-binding and chromatin localization properties of CHD1. *Mol. Cell. Biol.*, **15**, 2745–2753.
33. McKnight,J.N., Jenkins,K.R., Nodelman,I.M., Escobar,T. and Bowman,G.D. (2011) Extranucleosomal DNA binding directs nucleosome sliding by Chd1. *Mol. Cell. Biol.*, **31**, 4746–4759.
34. Wu,S.C. and Wong,S.L. (2005) Engineering soluble monomeric streptavidin with reversible biotin binding capability. *J. Biol. Chem.*, **280**, 23225–23231.
35. Magalhães,M.L., Czekster,C.M., Guan,R., Malashkevich,V.N., Almo,S.C. and Levy,M. (2011) Evolved streptavidin mutants reveal key role of loop residue in high-affinity binding. *Protein Sci.*, **20**, 1145–1154.
36. Patel,A., McKnight,J.N., Genzor,P. and Bowman,G.D. (2011) Identification of residues in chromo-helicase-DNA-binding protein 1 (Chd1) required for coupling ATP hydrolysis to nucleosome sliding. *J. Biol. Chem.*, **286**, 43984–43993.
37. Studier,F.W. (2005) Protein production by auto-induction in high density shaking cultures. *Protein Expr. Purif.*, **41**, 207–234.
38. Saha,A., Wittmeyer,J. and Cairns,B.R. (2002) Chromatin remodeling by RSC involves ATP-dependent DNA translocation. *Genes Dev.*, **16**, 2120–2134.
39. Puig,O., Caspary,F., Rigaut,G., Rutz,B., Bouveret,E., Bragado-Nilsson,E., Wilm,M. and Seraphin,B. (2001) The tandem affinity purification (TAP) method: a general procedure of protein complex purification. *Methods*, **24**, 218–229.
40. Luger,K., Rechsteiner,T.J. and Richmond,T.J. (1999) Expression and purification of recombinant histones and nucleosome reconstitution. *Methods Mol. Biol.*, **119**, 1–16.
41. Dyer,P.N., Edayathumangalam,R.S., White,C.L., Bao,Y., Chakravarthy,S., Muthurajan,U.M. and Luger,K. (2004) Reconstitution of nucleosome core particles from recombinant histones and DNA. *Methods Enzymol.*, **375**, 23–44.
42. Shahian,T. and Narlikar,G.J. (2012) Analysis of changes in nucleosome conformation using fluorescence resonance energy transfer. *Methods Mol. Biol.*, **833**, 337–349.
43. Lowary,P.T. and Widom,J. (1998) New DNA sequence rules for high affinity binding to histone octamer and sequence-directed nucleosome positioning. *J. Mol. Biol.*, **276**, 19–42.
44. Routh,A., Sandin,S. and Rhodes,D. (2008) Nucleosome repeat length and linker histone stoichiometry determine chromatin fiber structure. *Proc. Natl Acad. Sci. USA*, **105**, 8872–8877.
45. Kassabov,S.R. and Bartholomew,B. (2004) Site-directed histone-DNA contact mapping for analysis of nucleosome dynamics. *Methods Enzymol.*, **375**, 193–210.
46. Kassabov,S.R., Henry,N.M., Zofall,M., Tsukiyama,T. and Bartholomew,B. (2002) High-resolution mapping of changes in histone-DNA contacts of nucleosomes remodeled by ISW2. *Mol. Cell. Biol.*, **22**, 7524–7534.
47. Green,N.M. (1975) Avidin. *Adv. Protein Chem.*, **29**, 85–133.
48. Saha,A., Wittmeyer,J. and Cairns,B.R. (2005) Chromatin remodeling through directional DNA translocation from an internal nucleosomal site. *Nat. Struct. Mol. Biol.*, **12**, 747–755.
49. Schwanbeck,R., Xiao,H. and Wu,C. (2004) Spatial contacts and nucleosome step movements induced by the NURF chromatin remodeling complex. *J. Biol. Chem.*, **279**, 39933–39941.
50. Zofall,M., Persinger,J., Kassabov,S.R. and Bartholomew,B. (2006) Chromatin remodeling by ISW2 and SWI/SNF requires DNA translocation inside the nucleosome. *Nat. Struct. Mol. Biol.*, **13**, 339–346.
51. Imbalzano,A.N., Schnitzler,G.R. and Kingston,R.E. (1996) Nucleosome disruption by human SWI/SNF is maintained in the absence of continued ATP hydrolysis. *J. Biol. Chem.*, **271**, 20726–20733.
52. Logie,C. and Peterson,C.L. (1997) Catalytic activity of the yeast SWI/SNF complex on reconstituted nucleosome arrays. *EMBO J.*, **16**, 6772–6782.
53. Guyon,J.R., Narlikar,G.J., Sullivan,E.K. and Kingston,R.E. (2001) Stability of a human SWI-SNF remodeled nucleosomal array. *Mol. Cell. Biol.*, **21**, 1132–1144.
54. Lorch,Y., Cairns,B.R., Zhang,M. and Kornberg,R.D. (1998) Activated RSC-nucleosome complex and persistently altered form of the nucleosome. *Cell*, **94**, 29–34.
55. Kwon,H., Imbalzano,A.N., Khavari,P.A., Kingston,R.E. and Green,M.R. (1994) Nucleosome disruption and enhancement of activator binding by a human SW1/SNF complex. *Nature*, **370**, 477–481.
56. Guyon,J.R., Narlikar,G.J., Sif,S. and Kingston,R.E. (1999) Stable remodeling of tailless nucleosomes by the human SWI-SNF complex. *Mol. Cell. Biol.*, **19**, 2088–2097.
57. Lorch,Y., Maier-Davis,B. and Kornberg,R.D. (2010) Mechanism of chromatin remodeling. *Proc. Natl Acad. Sci. USA*, **107**, 3458–3462.
58. Gottschalk,A.J., Timinszky,G., Kong,S.E., Jin,J., Cai,Y., Swanson,S.K., Washburn,M.P., Florens,L., Ladurner,A.G., Conaway,J.W. *et al.* (2009) Poly(ADP-ribosyl)ation directs recruitment and activation of an ATP-dependent chromatin remodeler. *Proc. Natl Acad. Sci. USA*, **106**, 13770–13774.
59. Ahel,D., Horejsí,Z., Wiechens,N., Polo,S.E., Garcia-Wilson,E., Ahel,I., Flynn,H., Skehel,M., West,S.C., Jackson,S.P. *et al.* (2009) Poly(ADP-ribose)-dependent regulation of DNA repair by the chromatin remodeling enzyme ALC1. *Science*, **325**, 1240–1243.
60. Pines,A., Vrouwe,M.G., Marteijn,J.A., Typas,D., Luijsterburg,M.S., Cansoy,M., Hensbergen,P., Deelder,A., de Groot,A., Matsumoto,S. *et al.* (2012) PARP1 promotes nucleotide excision repair through DDB2 stabilization and recruitment of ALC1. *J. Cell Biol.*, **199**, 235–249.
61. Cairns,B.R. (2007) Chromatin remodeling: insights and intrigue from single-molecule studies. *Nat. Struct. Mol. Biol.*, **14**, 989–996.